Available online at www.sciencedirect.com
ScienceDirect
Polymer 47 (2006) 6684–6691
polymer
www.elsevier.com/locate/polymer

# Melt intercalation/exfoliation of polystyrene–sodium-montmorillonite nanocomposites using sulfonated polystyrene ionomer compatibilizers

Nikhil N. Bhiwankar [a,1], R.A. Weiss [a,b,*]

[a] Polymer Program, University of Connecticut, Storrs, CT 06269-3136, USA
[b] Department of Chemical Engineering, University of Connecticut, Storrs, CT 06269-3136, USA

Received 22 January 2006; received in revised form 10 July 2006; accepted 11 July 2006
Available online 14 August 2006

**Abstract**

Quaternary ammonium salts of sulfonated polystyrene (SPS) were used as compatibilizers for melt intercalation of PS and pristine Na-montmorillonite. Tetra-octyl ammonium SPS and tetra-decyl ammonium SPS ionomeric compatibilizers produced significant exfoliation and a homogeneous dispersion of the polymer–clay nanocomposites. Wide angle X-ray diffraction and transmission electron microscopy were primarily used to characterize the morphology of the nanocomposites. Image analysis was used to measure the percentage exfoliation. Exfoliation increased with the increasing length of the alkyl chain of the ammonium counter-ion of the SPS ionomer. The nanocomposites containing ionomers exhibited higher storage moduli compared to nanocomposites without the compatibilizer.
© 2006 Elsevier Ltd. All rights reserved.

*Keywords:* Nanocomposites; Ionomers; Clay

## 1. Introduction

Polymer-layered silicate nanocomposites (PLSNs) have generated significant interest in academia and industry as a result of their enhancement of a wide range of properties. PLSNs have been fabricated using different polymer matrices and various methods of preparation. The primary reason for the improvement of the material performance is incorporation and dispersion of highly anisotropic nanoscale reinforcements compared with conventional particulate microscale fillers. The properties of nanocomposites are determined not only by the characteristics of the individual components but also by the morphology formed [1]. The reinforcements in PLSNs are inorganic filler particles such as layered silicates. The literature on this class of materials is now quite extensive and includes a monograph [2] and a couple of recent review articles [3,4].

Layered silicates, such as sodium-montmorillonite (Na-Mmt), are commonly used as the inorganic filler. Their crystal lattice consists of two-dimensional layers, where a central octahedral sheet of alumina or magnesia is fused with two external silica tetrahedra at the tip [5]. The layer thickness of the sheets is around 1 nm. These layers organize into stacks with a regular Van der Waals gap called the 'interlayer' having a spacing of 0.96 nm. Isomorphous substitution of the $Al^{3+}$ by $Mg^{2+}$ or $Si^{4+}$ by $Al^{3+}$ within the silicate layer generates a net negative charge on the layer, which is counterbalanced by alkali or alkaline earth metal cations in the galleries. The interlamellar cations have one or two shells of water of hydration surrounding them; e.g. montmorillonite has the chemical formula $[M_x\ (Al_{4-x}Mg_x)\ Si_8O_{20}\ (OH)_4]$, where 'M' is a monovalent cation which resides in the intergallery spaces, and '$x$' is the degree of isomorphous substitution. There are several layers of organization within the clay minerals [6,7]. The typical particle size is 8–10 μm which comprises the tactoids. The smallest primary particles are stacks of parallel

* Corresponding author. Department of Chemical Engineering, Institute of Materials Science, University of Connecticut, 97 North Eagleville Road, Storrs, CT 06269-3136, USA. Tel.: +1 860 486 4698; fax: +1 860 486 6048.
*E-mail address:* rweiss@ims.uconn.edu (R.A. Weiss).
[1] Current address: Saint-Gobain High Performance Materials, Northboro Research and Development Center, 9 Goddard Road, Northborough, MA-01532, USA.

0032-3861/$ - see front matter © 2006 Elsevier Ltd. All rights reserved.
doi:10.1016/j.polymer.2006.07.017

lamellae with an average of 15–20 sheets per particle and of the order of 0.1–1 μm.

The most common strategies for fabricating PLSNs are *in situ*-polymerization [8,9], solution intercalation [10,11] and melt intercalation [12,13]. Melt intercalation is the most versatile and environmentally benign method that can be used for the commercial production of PLSNs. In this method, a mixture of polymer and silicate, heated above the glass transition or melting temperature of the polymer, is mixed using shear forces in an extruder. However, the silicates used in this method are usually surface modified to improve their interactions with hydrophobic polymers, which are mostly non-polar. Organic modification is achieved by exchanging the interlamellar alkali/alkaline ions with long chain alkyl amines or quaternary ammonium ions. But, organic modification has its own disadvantages. It not only requires an extra step in producing polymer/clay nanocomposites, but the organic modifiers commonly used degrade at the elevated temperatures needed to process the nanocomposites and thus cause the silicate layers to regain their hydrophilicity [14–16]. Instability of the organoclay can also adversely affect the stability of the polymer [17–19].

Though different polymers have been used as polymer matrices, there are limited reports of charged polymers such as ionomers being used in PLSNs. In the majority of studies using ionomers, organically modified montmorillonite was employed as the filler material [20–25]. We recently reported on the use of quaternary alkyl ammonium-neutralized sulfonated polystyrene ionomers for promoting intercalation in pristine Na-Mmt, with no organic modification [26]. Quaternary alkyl ammonium pendant groups on the hydrophobic polymer backbone of PS provide amphiphilic character to the polymer and, hence, are attractive for intercalating hydrophilic smectite clays. The approach of using ionomers as compatibilizers increased the silicate gallery spacing of pristine montmorillonite and produced partially intercalated/exfoliated morphologies [26]. There were two main objectives of the current study reported herein. The first goal was to examine the efficiency of various quaternary alkyl ammonium-neutralized SPS for promoting intercalation of the ionomer into unmodified Na-Mmt clay and its use as a compatibilizer for improving dispersion of the clay in another non-polar polymer such as PS. The effect of the length of alkyl substituents of the counter-ion on intercalation/exfoliation capability was evaluated. The second goal was to characterize the dynamic, mechanical and thermal properties of the composites. In our earlier work [26] we showed that an increase in the intergallery spacings occurred only when the ratio of the ion-exchange capacity and the cation exchange capacity, IEC/CEC $> 1$. In all the blends studied here, the amount of ionomers added in the extruder or the IEC of ionomers used is such that this criterion was met.

## 2. Experimental

### 2.1. Materials and synthesis

A commercial atactic polystyrene, Styron® 666, with $M_w = 280$ kDa and $M_n = 106$ kDa was provided by Dow Chemical Company and used as received. Sulfonated polystyrene (SPS) ionomers were prepared by sulfonating polystyrene (PS) in 1,2 dichloroethane solution using acetyl sulfate at 50 °C following the procedure of Makowski et al. [27]. The sulfonation reaction is an electrophilic substitution reaction, which substitutes sulfonic acid groups randomly along the chain, primarily at the para-position of the phenyl ring. The ionomers were isolated from solution by distillation of the solvent, filtered, washed several times with deionized distilled water, and dried under vacuum. The sulfonation level of the ionomer was determined by titration of the sulfonic acid derivative (HSPS) in a mixed solvent of toluene/methanol (90/10 v/v) with methanolic sodium hydroxide of known normality to a phenolphthalein end-point. Ionomers with three different counter-ions of varying alkyl chain lengths were prepared. Ionomers with mol% sulfonation between 8 and 9 were targeted in this study. The actual mol% sulfonation was 8.3.

Reagent grade *tert*-butyl ammonium hydroxide (Te-BuA), *tert*-octyl ammonium bromide (Te-OcA), and *tert*-decyl ammonium bromide (Te-DeA) were obtained from Aldrich Chemical Company and used as received. The alkyl ammonium salts of SPS were prepared by dissolving the HSPS in toluene/methanol solution and neutralizing them with stoichiometric addition of the appropriate alkyl ammonium salt. The reaction was allowed to progress for 12 h. The neutralized ionomers were isolated by steam distillation, filtered, washed several times with deionized distilled water and dried under vacuum at 80 °C. The sodium-montmorillonite (Na-Mmt) used was Cloisite $Na^+$, obtained from Southern Clay Products. CEC cited by the manufacturer was 0.92 meq/g and the clay was used as received without any further drying.

The sample nomenclature used for the ionomer in this article is *rst*-SPS*x*, where *rst* denotes the alkyl ammonium cation and *x* indicates the ion-exchange capacity (IEC) of the ionomer in meq/g. The sample nomenclature used for the quaternary salts was TeBu–SPS*x*, TeOc–SPS*x* and TeDe–SPS*x* for the tetra-butyl ammonium SPS, tetra-octyl ammonium SPS and tetra-decyl ammonium SPS, respectively.

### 2.2. Melt processing

A DACA micro-compounder (a vertical, recirculating co-rotating twin screw extruder) produced by DACA instruments, California, USA was used for melt processing SPS/PS/Na-Mmt blends. The extrusion temperature was 50 °C above the glass transition temperature ($T_g$), screw speed was 190 rpm and the mixing time was fixed at 10 min. The screw speed and mixing time were optimized after several trial runs. Polymers were added to the extruder using a lower screw speed (70 rpm) than was used for melt mixing with the clay. First, half of the polymer (~2 g) was added, followed by the addition of Na-Mmt after the polymer became molten. Then the remainder of the polymer was added and the screw speed was increased to 150 rpm. During mixing, the exit valve was closed and the recirculation valve was opened, so that the micro-compounder functioned as a batch mixer. After 10 min of mixing, samples were pumped out through the exit valve.

Any material left after that was removed from the screws and the barrel after stopping the extruder.

### 2.3. Materials characterization

Film samples (1 mm thick) for materials characterization were prepared by compression molding with a Wabash two-platen press using a rectangular mold at the same temperatures as the extrusion temperatures of the blends. A preheating time of 3 min without pressure was followed by a compression molding time of 5 min at higher pressure (~90 kN). The samples were water-cooled in the press at elevated pressure and removed from the press at room temperature. The blend nomenclature followed in this paper is (*m*/*n*)PS/*rst*-SPS*x*/Mmt for the PS/ionomer/Na-Mmt blends, where (*m*/*n*) denotes the PS/SPS*x* composition (w/w) based on the total polymer content. The composition of the silicate was fixed at 3 wt% of the total polymer mass, except for one sample that had 10 wt% silicate. The composite samples studied are summarized in Table 1.

Wide angle X-ray diffraction (WAXD) of compression molded specimens was done with a Bruker D8 Advance diffractometer using CuK$\alpha$ ($\lambda = 0.154$ nm) radiation at a voltage and current of 40 kV and 40 mA, respectively. The scattering angle ($2\theta$) was scanned at room temperature from 3° to 12° at a scan speed of 0.1°/min. This angular range corresponded to values of the momentum transfer vector $q = 4\pi \sin\theta/\lambda$ from 2.1 to 8.5 $nm^{-1}$. The basal spacing of the silicate layers ($d$) was calculated using Bragg's law $d = 2\pi/q$.

Transmission electron microscopy (TEM) was carried out with a Philips 300 electron microscope using an operating voltage of 80 kV. Thin sections (~70 nm) were microtomed from compression molded samples at room temperature with a diamond knife using an LKB ultramicrotome. The sections were collected from a water trough and floated directly onto Cu grids. The silicate layers are comprised of heavier elements, such as Si and Al, than the interlayer and surrounding matrix which are comprised of C, H, N and O, which provided sufficient contrast between the clay (darker objects in the TEM images) and the polymer, so no external staining was needed. Although natural contrast was adequate to resolve the clay from the polymer, the contrast was not sharp enough at all magnifications to utilize automated image analysis software to resolve single platelets from stacks of 2–3 platelets. As a result, the number of platelets per particle was counted manually. TEM specimens were viewed under a magnification range of 40K–120K so as to include a large number of platelets or agglomerates, which provided good statistics of the distribution of particle sizes. For each sample, 15–20 micrographs were analyzed to determine the total number of platelets and the average number of platelets per stack. The platelets were categorized as single platelets, stacks of 2–5 platelets and stacks comprising of more than 10 platelets. The percent exfoliation was defined as the percentage of single platelets in the population.

The glass transition temperature ($T_g$) and change in the specific heat ($\Delta C_p$) at the glass transition were measured with a temperature-modulated differential scanning calorimeter (TMDSC) (MDSC™, TA2920, TA Instruments) using a heating rate of 2.5 °C/min, a 60 s period heating/cooling cycle of modulation and an oscillation amplitude of ±1 °C. Dynamic mechanical properties of the composites were measured with a TA Instruments DMA model 2980 using the tensile mode and a frequency of 1 Hz. The mechanical properties were obtained on compression molded samples. The temperature range used was −60 °C to 130 °C, the amplitude of vibration was 10 μm and the heating rate was 2 °C/min.

## 3. Results and discussions

### 3.1. WAXD and TEM

Fig. 1 shows the WAXD data ($2\theta = 3$–$10°$) for PS/SPS/Na-Mmt composites as a function of alkyl chain length of the quaternary ammonium counter-ions in ammonium-neutralized SPS; each composite contained 3 wt% silicate. The diffraction patterns are offset vertically for clarity. The 150 °C XRD pattern of Na-Mmt shows that the base gallery spacing for the clay was 0.96 nm. The original $d_{001}$ spacing of Na-Mmt at room temperature is 1.03 nm; the difference is because of collapsing of the layers due to loss of water at high temperatures. The PLNs were processed between 150 and 160 °C, so it was assumed that the weakly bonded water in Na-Mmt was already lost from the clay.

The WAXD of the PS/silicate sample shows a peak at the same position as for the neat silicate that corresponds to a gallery spacing of 0.96 nm. The peak moved to lower $q$ for the PS/ionomer/silicate nanocomposites, which indicates higher spacings for the Na-Mmt galleries. The WAXD peak for the (75/25)PS/TeBu–SPS0.75/Mmt corresponded to a $d$-spacing of 1.37 nm, and the $d_{(001)}$ reflection of the (90/10)PS/TeOc–SPS0.75/Mmt composite, which exhibited the maximum

Table 1
Nomenclature and details of blend compositions

| Material | Counter-ion | IEC (meq/g) | wt% Silicate in blend | wt% PS in polymer content | Blend nomenclature |
|---|---|---|---|---|---|
| PS | – | 0 | 3 | 100 | (100/0)PS/Mmt |
| TeBu–SPS0.75 | Tetrabutyl ammonium | 0.75 | 3 | 75 | (75/25)PS/TeBu–SPS0.75/Mmt |
| TeOc–SPS0.75 | Tetraoctyl ammonium | 0.75 | 3 | 75 | (75/25)PS/TeOc–SPS0.75/Mmt |
| TeOc–SPS0.75 | Tetraoctyl ammonium | 0.75 | 3 | 90 | (90/10)PS/TeOc–SPS0.75/Mmt |
| TeOc–SPS0.75 | Tetraoctyl ammonium | 0.75 | 10 | 75 | (75/25)PS/TeOc–SPS0.75/Mmt-10 |
| TeDe–SPS0.75 | Tetradecyl ammonium | 0.75 | 3 | 75 | (75/25)PS/TeDe–SPS0.75/Mmt |

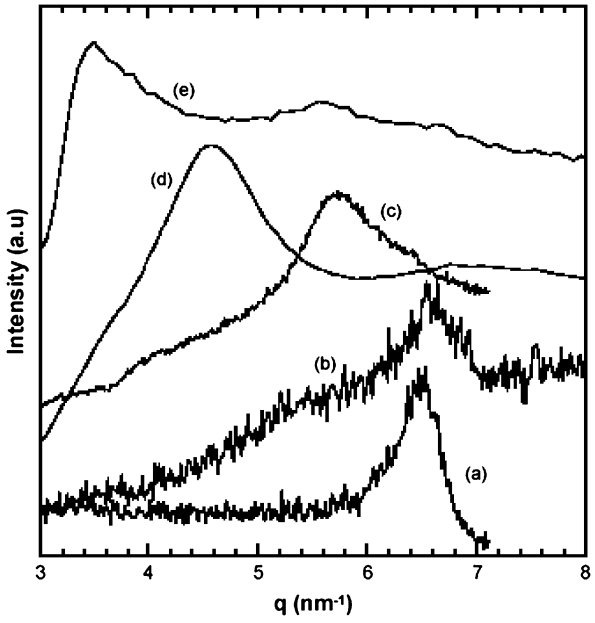


Fig. 1. WAXD of PS/SPS/Na-Mmt composites as a function of alkyl chain lengths of quaternary ammonium counter-ions in sulfonated PS ionomers, (a) Na-Mmt at 150 °C, (b) (100/0)PS/SPS/Mmt, (c) (75/25)PS/TeDe–SPS0.75/Mmt, (d) (75/25)PS/TeBu–SPS/0.75/Mmt, and (e) (90/10)PS/TeOc–SPS0.75/Mmt.

intercalation, shifted from 0.96 nm for Na-Mmt to 1.96 nm for the composite. Higher order reflections were not observed for any of these nanocomposites. The peak at $q \sim 5.5\ \mathrm{nm}^{-1}$ seen in curve (e) is a result of partial intercalation in some silicate layers, while the peak at $q \sim 6.8\ \mathrm{nm}^{-1}$ is presumably due to completely unintercalated layers. The peak position in curve (b) is similar to that of Na-Mmt (curve a) by itself. The large full width half maxima of the peaks indicate large inhomogeneities of intergallery spacings, though the positions of WAXD peaks were reproducible for different batches of nanocomposites with the same composition. For comparison, the changes in the *d*-spacings of Na-Mmt when an equivalent amount of low molecular weight quaternary ammonium salt such as Te-OcA was added in the extruder during melt mixing of PS and Na-Mmt was evaluated. In that case, the $d_{(001)}$ spacing changed from 0.96 to 1.09 nm compared with the 1.96 nm spacing observed when the TeOc–SPS ionomer was used.

A typical TEM bright field image of a (75/25)PS/TeOc–SPS0.75/Mmt nanocomposite at a relatively low magnification is shown in Fig. 2. Single clay layers, evidence for exfoliation, are present in abundance throughout the polymer matrix. However, intercalated and disordered layers also co-exist with the exfoliated silicate. There was no significant orientation of these platelets, as expected for a compression molded sample. The intercalated tactoids are responsible for the peak seen in the WAXD patterns while the disordered and exfoliated structures should have little or no contribution to the WAXD pattern over the angular range shown in Fig. 1. Some regions in the micrograph shown in Fig. 2, such as the feature marked (A) contained as many as 10–20 silicate layers stacked together. However, majority of the clay layers were present

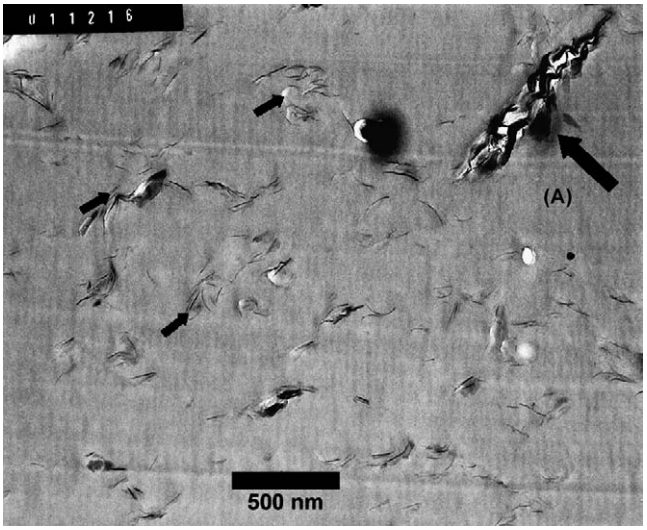


Fig. 2. TEM bright field image of (75/25)PS/TeOc–SPS0.75/Mmt containing 3 wt% silicate. The micrograph shows the co-existence of exfoliated layers (small arrows) and intercalated tactoids such as (A).

as single layers or as stacks of 2–5 layers (see the features marked by the small arrows in Fig. 2). The exfoliated layers had different lengths, with the average length between 80 and 140 nm. This disparity in platelet lengths may be due to a variety of reasons. First, clay platelets at the source of origin exhibit a wide distribution of lateral dimensions [28]. During extrusion of polymer–clay composites, the shear forces acting on the platelets may break them, which will further affect the distribution of sizes and shapes. In addition, the microtoming procedure may increase the heterogeneity in platelet length and thickness [29].

For the intercalated nanocomposites, the intercalated regions were more prevalent near the primary particle–polymer boundary. This was also observed in organically modified Mmt by Vaia et al. [7]. The flexibility of the layers due to their large aspect ratio and nm-thickness is clearly demonstrated by their curvature observed in Fig. 2. Similar mixed morphologies of intercalated and exfoliated clay were also observed in the other PS/ionomers nanocomposites that were studied here. In contrast, when mixing only PS with the silicate, i.e., without the addition of any ammonium-neutralized ionomer, only large agglomerates or 'tactoids' of clay were observed. This further corroborated the compatibilizing effect of the ionomers at dispersing Na-Mmt in these nanocomposites. The TEM micrographs shown in Fig. 3 compare the morphologies of the PS/SPS/clay nanocomposites. These images emphasize the excellent nano to microscale dispersion of pristine Na-Mmt without the aid of any organic modification in the compounds containing the ammonium-neutralized ionomers.

Image analysis (15–20 images for each sample were analyzed) of the particles in TEM micrographs was done to determine the distribution of silicate layers per particle. Fig. 4 shows a histogram of the distribution, broken up into single platelets, stacks of 2–5 layers, stacks of 6–10 layers and stacks containing more than 10 platelets. Since all compounds contained the same amount of clay (3 wt%), the total number

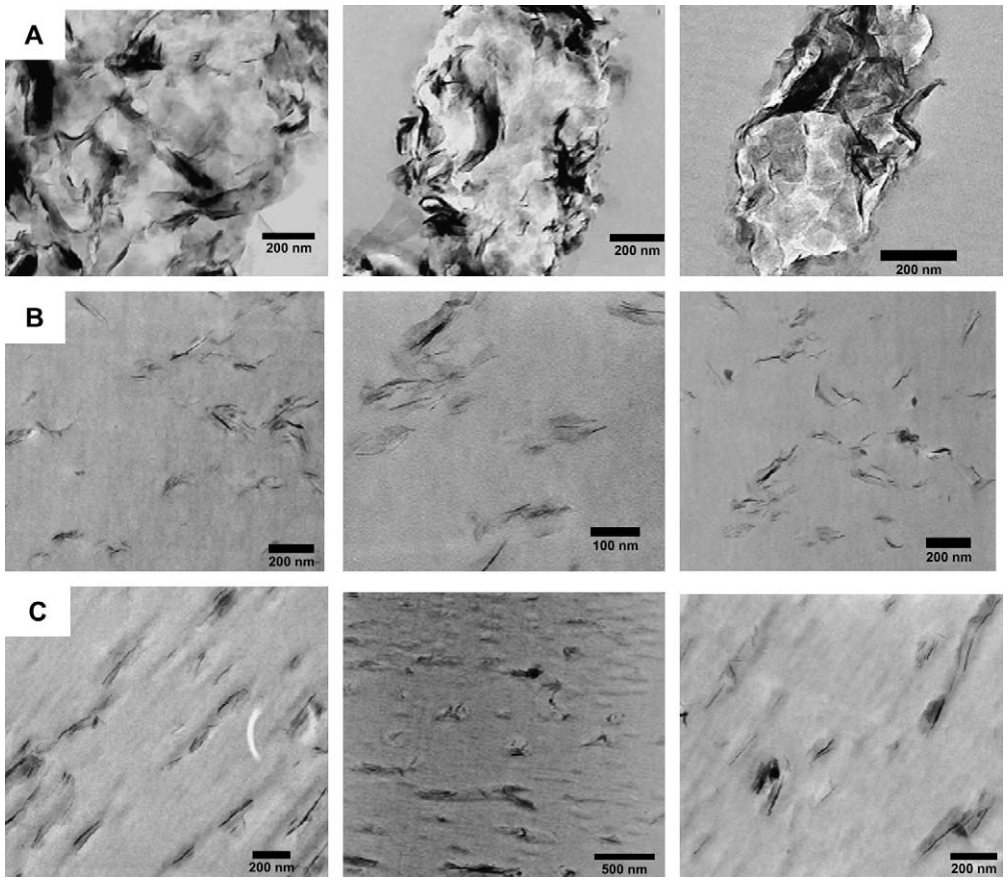


Fig. 3. Representative TEM micrographs taken at different magnifications. (A) (100/0)PS/SPS/Na-Mmt, (B) (90/10)PS/TeOc–SPS0.75/Mmt, and (C) (75/25)PS/TeDe–SPS0.75/Mmt.

of single platelets and stacks reflects the degree of dispersion in these composites, i.e., the higher the number of platelets and stacks, the better dispersed and delaminated was the clay. (75/25)PS/TeOc–SPS0.75/Mmt, (90/10)PS/TeOc–SPS0.75/Mmt and (75/25)PS/TeDe–SPS0.75/Mmt had a much larger percentage of single platelets than the (100/0)PS/SPS/Mmt composite. Depending on the percent contribution of single platelets, the various nanocomposites were classified as exfoliated/intercalated or immiscible. The histogram for (100/0)PS/SPS/Mmt composite had no tactoids smaller than 10 platelets, and that nanocomposite was considered to be immiscible. The ionomer-compatibilized nanocomposites exhibited 65–80% exfoliation depending on the counter-ion used to neutralize the ionomers, and those compounds were considered exfoliated/intercalated. Although the statistics for the compounds that used the TeOc and TeDe-ammonium ionomers are probably not significantly different to allow any conclusions as to the effect of the longer alkyl chain lengths of the counter-ion on exfoliation, both were significantly better at compatibilizing the clay than the TeBu-ammonium ionomer.

The lack of substantial exfoliation in the composites containing TeBu–SPS0.75 ionomer compared to the TeOc and TeDe salts suggests that an optimum level of interlayer separation is essential to achieve exfoliated morphologies. One might expect that nanocomposites with ionomers having quaternary counter-ions with shorter alkyl chains such as tetrabutyl ammonium should exchange easily with $Na^+$ in the intergalleries, but the smaller cation is also expected to provide the lowest reduction of the cohesive forces between adjacent platelets and, therefore, the smallest change in the gallery spacing. The tetrabutyl ammonium ion between the galleries

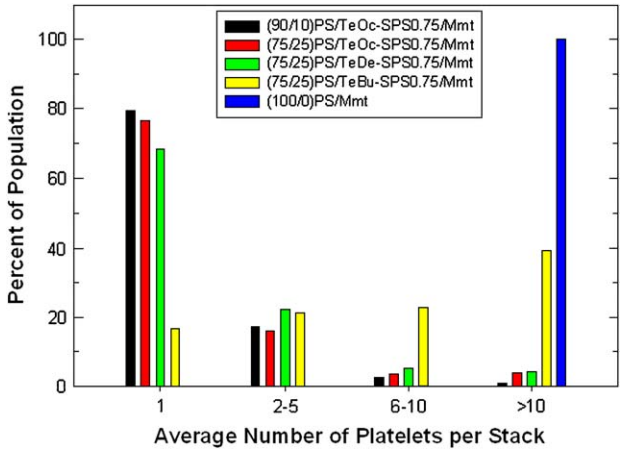


Fig. 4. Histogram of number of platelets per particle of (a) (100/0)PS/SPS/Mmt, (b) (75/25)PS/TeDe–SPS0.75/Mmt, (c) (75/25)PS/TeOc–SPS0.75/Mmt, (d) (90/10)PS/TeOc–SPS0.75/Mmt, and (e) (75/25) PS/TeBu–SPS0.75/Mmt.

will mask a relatively small amount of silicate surface from the polymer chain, which would lead to more unfavorable contacts of the polymer chains with the silicate surface. The better degree of exfoliation (65–80%) using the TeOc- and TeDe-ionomers may be due to the strong driving force for intercalation provided by ion exchange of $Na^+$ in the galleries with the quaternary ammonium ions on the polymer chain. The initial intercalation of the ammonium ions swells the galleries, decreasing the interlayer interactions and thus facilitating the penetration by the polymer at the edges of clay particles.

### 3.2. Thermal properties

Addition of an inorganic filler to a polymer can affect the thermal properties such as $T_g$ and melting point. There are contradictory conclusions in the literature as to what changes in $T_g$ to expect for intercalated/exfoliated PLSNs. Some researchers have shown either slight [30] or large increases in $T_g$ [31], while others have shown no increase [32–34]. Chen et al. [35] report a decrease in $T_g$ for poly(ethylene oxide)/clay/$LiClO_4$ nanocomposites. There are also reports of an absence of a glass transition in neatly intercalated nanocomposites [36–39] at relatively high concentrations of the inorganic species.

The change in the heat capacity ($\Delta C_p$) for PLSNs at $T_g$ is reduced by the presence of inorganic clay particles [37]. In this study, modulated DSC (MDSC) was used to provide better resolution and sensitivity of the changes in $\Delta C_p$, as other researchers have reported difficulties in detecting changes in $T_g$ for clay nanocomposites [40] using conventional DSC. Table 2 compares transition temperatures for nanocomposites and PS/SPS polymer blends without clay. For the same composition, different samples were run at least in triplicate. There is no substantial difference in the $T_g$s of the filled and unfilled systems, except for the (75/25)PS/TeBu–SPS0.75/Mmt compound. This nanocomposite showed an increase in $T_g$ of ~8–9 °C over the unfilled blend. Although the TEM images and WAXD results indicate that intercalation and partial exfoliation of the silicate layers occurred in both (90/10)PS/TeOc–SPS0.75/Mmt and (75/25)PS/TeDe–SPS0.75/Mmt nanocomposites, no changes in the $T_g$ were observed for those compounds compared to the unfilled blends with the same polymer composition.

The intercalation of polymer in the intergalleries has been shown to reduce the $\Delta C_p$ [41]. The addition of 3 wt% clay, whether it was intercalated, exfoliated or not, had little or no effect on $\Delta C_p$ of the PS/SPS blends and clay nanocomposites. However, when a higher silicate composition, 10 wt%, was used, i.e., the (75/25)PS/TeOc–SPS0.75/Mmt-10 nanocomposite, $\Delta C_p$ decreased, as shown in Table 2. The reduction of $\Delta C_p$ for an amorphous polymer is usually due to lower mobility of the polymer chains, which might be expected in the more highly loaded and exfoliated compounds. This result is consistent with the report by Winberg et al. [42] for nanocomposites containing 10 wt% clay or higher.

### 3.3. Dynamic modulus

Exfoliated polymer silicate systems generally exhibit higher mechanical properties than the unfilled polymer [43], in addition to maintaining optical clarity due to nanoscale dispersion of the silicate layers. The effect of silicate reinforcement caused by molecular dispersion of the silicate layers on the modulus of these compounds was probed using DMA. Fig. 5a compares dynamic storage modulus curves of (75/25)PS/TeBu–SPS0.75/Mmt and (90/10)PS/TeOc–SPS0.75/Mmt with unfilled polymer blends. These unfilled polymer blends were prepared in the same way as the composites using DACA extruder, but without the addition of clay. The moduli of the PS/ionomer/clay nanocomposites were higher than those of the unfilled materials over the entire temperature range under investigation. This is seen more clearly from the ratio between storage modulus of the composite ($E'_{composite}$) to the storage modulus of unfilled polymer blend ($E'_{blend}$) as shown in Fig. 5a as a function of temperature.

Enhancement in the modulus was greater in the glass transition region and above $T_g$. The modulus enhancement below $T_g$ was about 20–40%, while above $T_g$ the improvement of the softer elastomeric matrix was as high as 90%. No improvement in stiffness was achieved in the immiscible blends of Na-Mmt in PS; in fact, the addition of the clay seemed to decrease the modulus. This may be a consequence of the poor and heterogeneous dispersion of the clay in PS. Data for a composite of PS/clay with the addition of a low molecular weight quaternary ammonium salt, Te-OA are also shown in Fig. 5b. That blend showed about a 10% modulus increase below the $T_g$, but the modulus dropped precipitously above 60 °C.

## 4. Conclusions

The length of the alkyl chain length used on the quaternary ammonium counter-ions in sulfonated polystyrene ionomers plays a major role in the ability of the ionomer to intercalate and exfoliate Na-montmorillonite clays. When mixed with polystyrene, the alkyl ammonium-neutralized ionomers prove to be effective compatibilizers for the dispersion and

Table 2
$T_g$ and $\Delta C_p$ values of filled and unfilled blends

| Sample | (75/25)PS/TeBu–SPS0.75/Mmt | | (75/25)PS/TeDe–SPS0.75/Mmt | | (75/25)PS/TeOc–SPS0.75/Mmt | | |
|---|---|---|---|---|---|---|---|
| wt% Clay | 0 | 3 | 0 | 3 | 0 | 3 | 10 |
| $T_g$ (°C) | 96.8 | 105.2 | 94.36 | 93.3 | 91.3 | 91.9 | 92.1 |
| Derivative heat capacity (J/g/°C/°C) | 0.2405 | 0.247 | 0.2042 | 0.1935 | 0.214 | 0.193 | 0.149 |

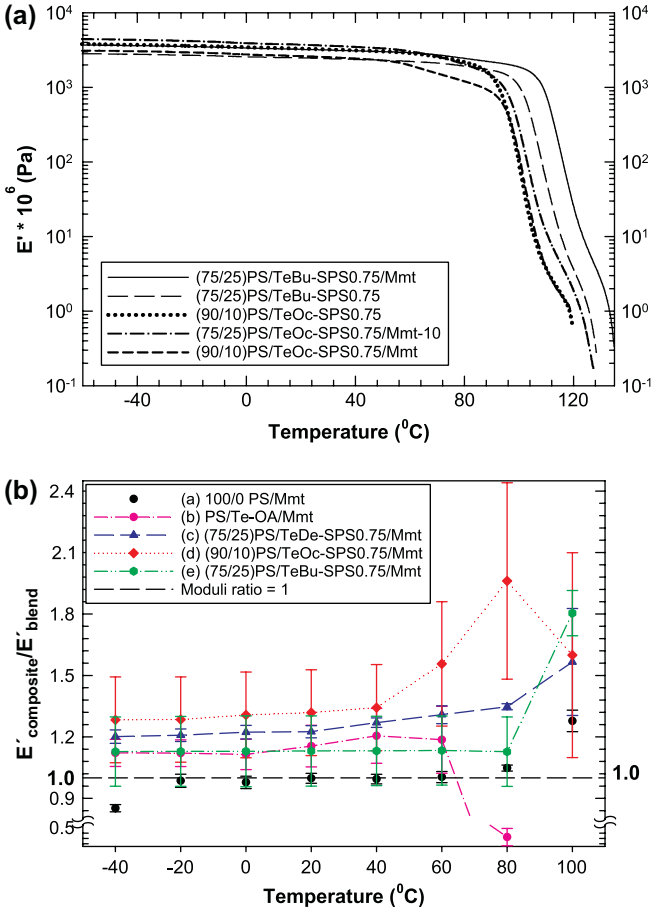


Fig. 5. (a) Dynamic storage moduli of PS/SPS/clay nanocomposites (3 wt% clay) and the corresponding unfilled polymer blend as a function of temperature. (b) Effect of temperature on the relative dynamic storage moduli ($E'_{composite}/E'_{blend}$) for the PS/SPS/clay nanocomposites (3 wt% clay).

exfoliation of the clay in nanocomposites. The percentage exfoliation depends on the extent of the platelet separation caused by the quaternary ammonium ion which exchanges with the $Na^+$ in the intergalleries. No increase in $T_g$ was observed for 60–80% ionomer/PS/clay nanocomposites with 60–80% of the clay exfoliated, but a nanocomposite wherein most of the clay was intercalated rather than exfoliated, i.e., (75/25)PS/TeBu–SPS0.75/Mmt showed a 8–9 °C increase in $T_g$. The dynamic storage modulus increased with the addition of clay for all the compatibilized nanocomposites, the PS/clay nanocomposites exhibited no increase in modulus compared with the unfilled polymer. Of the quaternary salts studied here tetra-octyl ammonium appeared to provide the best balance of exfoliation and improvement in the properties of the blends.

## Acknowledgments

This work was partially supported by grants from the Polymer Program of the National Science Foundation (Grant 0304803) and from NASA through the Connecticut Space Grant College Consortium. We are grateful to Prof. Robert Cohen at M.I.T. for the use of his DACA extruder for this research and his graduate student, Roger Aronow, for his assistance.

## References

[1] Paul DR, Newman S, editors. Polymer blends, vol. 1; 1978. p. 501.
[2] Pinnavaia TJ, Beall GW. Polymer–clay nanocomposites. 1st ed. Chichester: John Wiley and Sons, Ltd; 2000.
[3] Alexandre M, Dubois P. Polymer-layered silicate nanocomposites: preparation, properties and uses of a new class of materials. Mater Sci Eng Rep 2000;28(1–2):1–63.
[4] Biswas M, Ray SS. Recent progress in synthesis and evaluation of polymer-montmorillonite nanocomposites. Adv Polym Sci 2001;155: 167–221 (New polymerization techniques and synthetic methodologies).
[5] Theng BKG. The chemistry of clay-organic reactions. 1st ed. New York: Halsted Press; 1974.
[6] Vaia RA, Jandt KD, Kramer EJ, Giannelis EP. Kinetics of polymer melt intercalation. Macromolecules 1995;28(24):8080–5.
[7] Vaia RA, Jandt KD, Kramer EJ, Giannelis EP. Microstructural evolution of melt intercalated polymer-organically modified layered silicates nanocomposites. Chem Mater 1996;8(11):2628–35.
[8] Kojima Y, Usuki A, Kawasumi M, Okada A, Kurauchi T, Kamigaito O. One-pot synthesis of nylon 6-clay hybrid. J Polym Sci Part A Polym Chem 1993;31(7):1755–8.
[9] Usuki A, Kojima Y, Kawasumi M, Okada A, Fukushima Y, Kurauchi T, et al. Synthesis of nylon 6-clay hybrid. J Mater Res 1993;8(5):1179–84.
[10] Kawasumi M, Hasegawa N, Usuki A, Okada A. Nematic liquid crystal/clay mineral composites. Mater Sci Eng C 1998;6(1–2):135–43.
[11] Ogata N, Kawakage S, Ogihara T. Poly(vinyl alcohol)–clay and poly(ethylene oxide)–clay blends prepared using water as solvent. J Appl Polym Sci 1997;66(3):573–81.
[12] Vaia RA, Vasudevan S, Krawiec W, Scanlon LG, Giannelix EP. New polymer electrolyte nanocomposites. Melt intercalation of poly(ethylene oxide) in mica-type silicates. Adv Mater (Weinheim, Ger) 1995; 7(2):154–6.
[13] Dennis HR, Hunter DL, Chang D, Kim S, White JL, Cho JW, et al. Effect of melt processing conditions on the extent of exfoliation in organoclay-based nanocomposites. Polymer 2001;42(23):9513–22.
[14] VanderHart DL, Asano A, Gilman JW. Solid-state NMR investigation of paramagnetic nylon-6 clay nanocomposites. 2. Measurement of clay dispersion, crystal stratification, and stability of organic modifiers. Chem Mater 2001;13(10):3796–809.
[15] Xie W, Gao Z, Pan W-P, Hunter D, Singh A, Vaia R. Thermal degradation chemistry of alkyl quaternary ammonium montmorillonite. Chem Mater 2001;13(9):2979–90.
[16] Xie W, Gao Z, Liu K, Pan WP, Vaia R, Hunter D, et al. Thermal characterization of organically modified montmorillonite. Thermochim Acta 2001;367–368:339–50.
[17] Turner SR, Matabayas JJC. Nanocomposite technology for enhancing the gas barrier of polyethylene terephthalate. In: Pinnavaia TJ, Beall GW, editors. Polymer–clay nanocomposites. Chichester: John Wiley and Sons, Ltd; 2000. p. 207–25.
[18] Fornes TD, Yoon PJ, Paul DR. Polymer matrix degradation and color formation in melt processed nylon 6/clay nanocomposites. Polymer 2003;44(24):7545–56.
[19] Yoon PJ, Hunter DL, Paul DR. Polycarbonate nanocomposites: Part 2. Degradation and color formation. Polymer 2003;44(18):5341–54.
[20] Barber GD, Calhoun BH, Moore RB. Poly(ethylene terephthalate) ionomer based clay nanocomposites produced via melt extrusion. Polymer 2005;46(17):6706–14.
[21] Chisholm BJ, Moore RB, Barber G, Khouri F, Hempstead A, Larsen M, et al. Nanocomposites derived from sulfonated poly(butylene terephthalate). Macromolecules 2002;35(14):5508–16.
[22] Barber GD, Moore RB. Application of an ionomeric compatibilizer for organically-modified montmorillonite/PET nanocomposites. Polym Mater Sci Eng 2000;82:241–2.

[23] Parent JS, Liskova A, Resendes R. Isobutylene-based ionomer composites: siliceous filler reinforcement. Polymer 2004;45(24):8091–6.
[24] Shah RK, Hunter DL, Paul DR. Nanocomposites from poly(ethylene-*co*-methacrylic acid) ionomers: effect of surfactant structure on morphology and properties. Polymer 2005;46(8):2646–62.
[25] Kim BK, Seo JW, Jeong HM. Morphology and properties of waterborne polyurethane/clay nanocomposites. Eur Polym J 2002;39(1):85–91.
[26] Bhiwankar NN, Weiss RA. Melt-intercalation of sodium-montmorillonite with alkylamine and quarternized ammonium salts of sulfonated polystyrene ionomers. Polymer 2005;46(18):7246–54.
[27] Makowski HS, Lundberg RD, Singhal GH. Flexible plastic masses, 2348842; 1974.
[28] Fornes TD, Paul DR. Modeling properties of nylon 6/clay nanocomposites using composite theories. Polymer 2003;44(17):4993–5013.
[29] Cho JW, Paul DR. Nylon 6 nanocomposites by melt compounding. Polymer 2000;42(3):1083–94.
[30] Tyan H-L, Liu Y-C, Wei K-H. Thermally and mechanically enhanced clay/polyimide nanocomposite via reactive organoclay. Chem Mater 1999;11(7):1942–7.
[31] Agag T, Koga T, Takeichi T. Studies on thermal and mechanical properties of polyimide–clay nanocomposites. Polymer 2001;42(8):3399–408.
[32] Finnigan B, Martin D, Halley P, Truss R, Campbell K. Morphology and properties of thermoplastic polyurethane composites incorporating hydrophobic layered silicates. J Appl Polym Sci 2005;97(1):300–9.
[33] Wang ZM, Chung TC, Gilman JW, Manias E. Melt-processable syndiotactic polystyrene/montmorillonite nanocomposites. J Polym Sci Part B Polym Phys 2003;41(24):3173–87.
[34] Weon JI, Sue HJ. Effects of clay orientation and aspect ratio on mechanical behavior of nylon-6 nanocomposite. Polymer 2005;46(17):6325–34.
[35] Chen H-W, Chiu C-Y, Chang F-C. Conductivity enhancement mechanism of the poly(ethylene oxide)/modified-clay/$LiClO_4$ systems. J Polym Sci Part B Polym Phys 2002;40(13):1342–53.
[36] Frisch HL, Xue Y. Hybrid inorganic/organic interpenetrating polymer networks based on zeolite 13X and polystyrene. J Polym Sci Part A Polym Chem 1995;33(12):1979–85.
[37] Krishnamoorti R, Vaia RA, Giannelis EP. Structure and dynamics of polymer-layered silicate nanocomposites. Chem Mater 1996;8(8):1728–34.
[38] Strawhecker KE, Manias E. Structure and properties of poly(vinyl alcohol)/$Na^+$ montmorillonite nanocomposites. Chem Mater 2000;12(10):2943–9.
[39] Vaia RA, Sauer BB, Tse OK, Giannelis EP. Relaxations of confined chains in polymer nanocomposites: glass transition properties of poly(ethylene oxide) intercalated in montmorillonite. J Polym Sci Part B Polym Phys 1997;35(1):59–67.
[40] Verdonck E, Schaap K, Thomas LC. A discussion of the principles and applications of modulated temperature DSC (MTDSC). Int J Pharm 1999;192(1):3–20.
[41] Li Y, Ishida H. A study of morphology and intercalation kinetics of polystyrene–organoclay nanocomposites. Macromolecules 2005;38(15):6513–9.
[42] Winberg P, Eldrup M, Pedersen NJ, van Es MA, Maurer FHJ. Free volume sizes in intercalated polyamide 6/clay nanocomposites. Polymer 2005;46(19):8239–49.
[43] Kojima Y, Usuki A, Kawasumi M, Okada A, Kurauchi T, Kamigaito O. Synthesis of nylon 6-clay hybrid by montmorillonite intercalated with ε-caprolactam. J Polym Sci Part A Polym Chem 1993;31(4):983–6.